UDC 539.4

Flexural Fatigue Behavior of Cross-Ply Laminates: An Experimental Approach

A. R. Bezazi,[a] A. El Mahi,[b] J.-M. Berthelot,[b] and B. Bezzazi[c]

[a] Laboratoire de Mécanique et de Structure (LMS), Université 08 Mai 1945, Guelma, Algeria

[b] Institute of Acoustic and Mechanics Group of Composite and Mechanical Structures, University of Le Mans, Le Mans, France

[c] Institute of the Materials of Constructions, University of Boumerdes, Boumerdes, Algeria

УДК 539.4

Сопротивление усталости перекрестно-армированных ламинатов при изгибе

А. Р. Безази[а], А. Эль Махи[б], Дж.-М. Бертело[б], Б. Беззази[в]

[а] Университет г. Гуэльма, Алжир

[б] Университет г. Ле Манс, Франция

[в] Университет г. Бумэрди, Алжир

В рамках экспериментального подхода описано механическое поведение различных ламинатов с матрицей из эпоксидной смолы, перекрестно-армированных кевларовыми волокнами и стекловолокнами, в условиях статического и циклического трехточечного изгиба. При статических испытаниях рассматриваются последовательность укладки слоев и волокон, толщины слоев, ориентированных под углом 90°, и влияние типа армирования на механическое поведение ламинатов в процессе нагружения, а также на реализацию различных режимов повреждения, приводящих к разрушению. Исследования при циклическом нагружении состоят из двух этапов. На первом этапе изучается влияние последовательности укладки слоев и волокон на поведение и долговечность четырех типов ламинатов, армированных стекловолокнами, на втором этапе – влияние типа армирования на циклическую прочность и сопротивление ламинатов при циклическом нагружении. Усталостные испытания выполнены в мягком режиме нагружения для ламинатов, армированных стекловолокнами и гибридными волокнами (кевлар+стекло). Кривые усталости были построены в координатах напряжение – число циклов до разрушения на основе критериев снижения жесткости на 5 и 10%. Анализ полученных результатов позволяет оценить влияние последовательности укладки слоев и типа армирования на поведение перекрестно-армированных ламинатов при циклическом нагружении. Наличие кевларовых волокон в ламинатах обеспечивает их нелинейное поведение при статических испытаниях и низкую циклическую прочность при усталостных испытаниях в условиях трехточечного изгиба.

Ключевые слова: ламинаты, кевларовые волокна, гибридные волокна, эпоксидная матрица, трехточечный изгиб, усталость, повреждение, кривые усталости.

Introduction. Modern aerospace, aeronautical, naval, motor, and railway technologies require materials with high mechanical properties. However, the experience acquired in the use of homogeneous traditional materials showed their limited potential applications. Fortunately, the alternative appeared with composite materials whose properties are very interesting: lightness, high directional stiffness, good resistance to fatigue, the absence of corrosion for nonmetallic constituents, ease of fabrication, etc. Such materials, despite the misunderstanding of certain aspects of their behavior, have stimulated a great interest in several industrial applications. Over the last three decades, several investigations have been carried out on the fatigue behavior of composite materials with organic matrices (epoxy, polyester, etc.) and continuous fibers (glass, aramide, carbon, etc.) The prediction of their fatigue life, however, is still difficult to achieve thus necessitating a better understanding of many damage mechanisms that may lead to total rupture.

A great number of studies are reported in the literature on the traction and flexural fatigue of composite materials. The influence of fatigue behavior of the components of those materials was studied by several authors [1–3]. Mandell [4] described the process of rupture in fatigue in the case of tensile tests of glass fiber composites. It was shown that rupture depends only on the properties of the fibers independently of the matrix. In a review paper, Talreja [5] summarized various interpretations of damage mechanisms in fatigue of plastic matrix composites. Kim and Ebert [6] studied the influence of cycling frequency, via 4-point bending, on unidirectional glass fiber composites; they found that an increase in frequency leads to a rise in the material temperature without significant effects on fundamental fatigue mechanisms. They also put into evidence the influence of the distance between supporting points, l, on the rupture mechanisms. Djebar et al. [7] studied, via 3-point bending, the influence of the ratio l/h (where h is the specimen thickness) on the fatigue of glass/epoxy composites. Several other studies of composite materials and their damage behavior via 3- and 4-point bending and tension were also reported in [8–26].

Aramide (Kevlar) fibers possess high mechanical properties being 4 to 6 times cheaper than carbon fibers. Nevertheless, Kevlar fiber laminates have various weaknesses (weak compressive resistance to bending, to buckling, etc.) These weaknesses are generally attributed to a bad fiber-matrix adherence [27]. To overcome such a problem, hybrid composites (glass–Kevlar, carbon–Kevlar) are used. Only few investigations [28–33] are reported on Kevlar fibers and hybrids. In this context, we carry out an investigation in static and cyclic fatigue, using 3-point bending, on different cross-ply laminates made of epoxy resin and glass fibers, Kevlar fibers, and hybrid (glass–Kevlar) fibers.

Static tests are carried out on various laminated composites allowing the analysis of stacking sequence effects, of (0°- and 90°-oriented) layer thickness ratios, and of the reinforcement type on the behavior and on different types of damages up to laminate rupture. Fatigue investigations consist of two parts: (i) the influence of the stacking sequence on both the behavior and fatigue life of four types of glass-fiber laminates and (ii) determination of the reinforcement type effects on the laminate behavior and endurance. Hence, several glass fiber laminates and various loading ratios R are considered. Moreover, the endurance tests are performed not only with displacement control but also with load control

for Kevlar and glass fiber laminates. Stress vs number of cycles (S–N) endurance diagrams (Wцhler's curves) are plotted using the criteria of fatigue life N_5 and N_{10} corresponding, respectively, to 5% and 10% reduction in stiffness with respect to the initial value.

1. **Materials and Tests**.

1.1. **Materials**. Different cross-ply laminates were prepared by vacuum moulding from continuous glass fibers, Kevlar fibers, hybrid (glass–Kevlar) fibers, and epoxy resin. The obtained laminates differ by (i) the reinforcement type; (ii) the stacking sequence, and (iii) the (0°- and 90°-oriented) layer thickness ratios. Nine glass fiber laminates (GFL) consisting of 16 plies each and designated by GFL 1 to GFL 9 were investigated. A hybrid glass and Kevlar fiber laminate (HGKFL) consists of 8 plies of glass and 4 plies of Kevlar, and Kevlar-fiber laminate (KFL) consists of 8 plies. The choice of the number of glass and Kevlar plies is dictated by the necessity of keeping the specimen thickness almost constant. The ensemble of these laminates and their stacking sequences are grouped in Table 1. The important characteristics of laminate constituents are given in Tables 2 and 3 for epoxy resin SR 1500/SD 2505 and continuous fibers, respectively.

Table 1

Investigated Materials

GFL 1	GFL 2	GFL 3	GFL 4	GFL 5	GFL 6
$(90_4/0_4)_s$	$(0_4/90_4)_s$	$(90_6/0_2)_s$	$(0_6/90_2)_s$	$[(0_2/90_2)_s]_s$	$[(0/90)_4]_s$
GFL 7	GFL 8	GFL 9	HGKFL		KFL
$[(0_2/90_2)_2]_s$	$(90_2/0_6)_s$	$(0_2/90_6)_s$	$(0_{2v}/0_k/90_{2v}/90_k)_s$		$(0_{2k}/90_{2k})_s$

Table 2

Characteristics of Epoxy Resin SR 1500/SD 2505

Young's modulus (GPa)	Tensile strength (MPa)	Flexural strength (MPa)
2.9–3.2	74–77	115–120

Table 3

Characteristics of Kevlar and Glass Fibers

Reinforcement type	Surface mass (g/m^2)	Density (kg/m^3)	Young's modulus (GPa)	Shear modulus (GPa)	Poisson's ratio	Ultimate strength (MPa)	Elongation at rupture
Glass	300	2540	74	30	0.25	2500	4.8
Kevlar	400	1450	130	12	0.40	2900	2.6

The laminates are prepared in vacuum by moulding with the use of the so-called "technique of the bag" to obtain 300×300 mm wafers. The plies are laminated and impregnated at room temperature, then moulded under vacuum (30 kPa) for 10 hours. The wafers were cut out with a diamond tip disk saw according to standard ASTM D 790-8a.

1.2. **Tests**.

1.2.1. *Static Tests*. The investigation of specimens (Table 1) is carried out in 3-point bending (Fig. 1) using a universal hydraulic monotonic testing machine (INSTRON model 8516 of capacity 100 kN) whose control and data acquisition are performed by a computer. At least five tests are carried out for each type of laminates with a test speed of 2 mm/min.

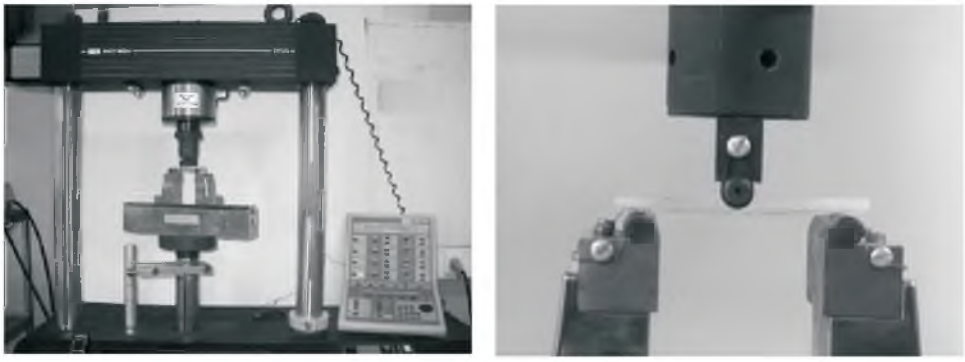

a *b*

Fig. 1. Experimental setup: (*a*) Instron 8516 servo-hydraulic testing machine; (*b*) specimen under 3-point bending test.

1.2.2. *Fatigue Tests*. Two types of tests types were carried out on specimens identical to those used in the previous static case with a sinusoidal waveform with a frequency of 10 Hz.

a) *First test type.*

These tests, carried out in displacement control, allow the determination of the influence of the stacking sequence on fatigue resistance. To do so, we considered the laminates GFL 2 $(0_4/90_4)$, GFL 5 $[(0_2/90_2)_s]_s$, GFL 6 $[(0/90)_4]_s$ and GFL 7 $[(0_2/90_2)_2]_s$ all of which possess the same number of plies at 0° and at 90° (the ratio of the layer thickness equals to 1). These laminates are piled up so that the thickness of the 90°-oriented layers is different. The loading level r ($r = d_{\max}/d_{rup}$), representing the ratio of the maximum displacement to the static rupture displacement, is taken to have a constant value of 60% of that of static rupture displacement. Several loading ratios, R, which is the ratio of the minimum and maximum displacements ($R = d_{\min}/d_{\max} = 0.1,\ 0.25,\ 0.4,\ 0.55,\ 0.7$) are considered.

b) *Second test type.*

These tests are carried out by considering two load types: (i) the first method consists of carrying out displacement control tests. The average displacement (d_{av}) is maintained constant at 40% of the static rupture displacement (d_{rup}). Several loading levels r are considered in order to plot Wцhler's curves for GFL 2 and HGKFL laminates, (ii) the second method is carried out in load control with a constant load ratio R equal to 0. To plot the endurance diagrams, we considered several loading levels ranging from 95% to 40% of the static rupture load for GFL 2 and KFL laminates.

2. **Results and Discussion**.

2.1. **Static Tests**. Figure 2 represents load evolution as a function of displacement for various tested laminates. The results are analyzed by grouping each time a number of laminates. This makes it possible to reveal the effects of (i) stacking sequence, (ii) the thickness and the interior or exterior disposition of the 0°- and 90°-oriented layers in the laminate, and (iii) finally, the type of the reinforcement on stiffness, load, and displacement at rupture of the laminate.

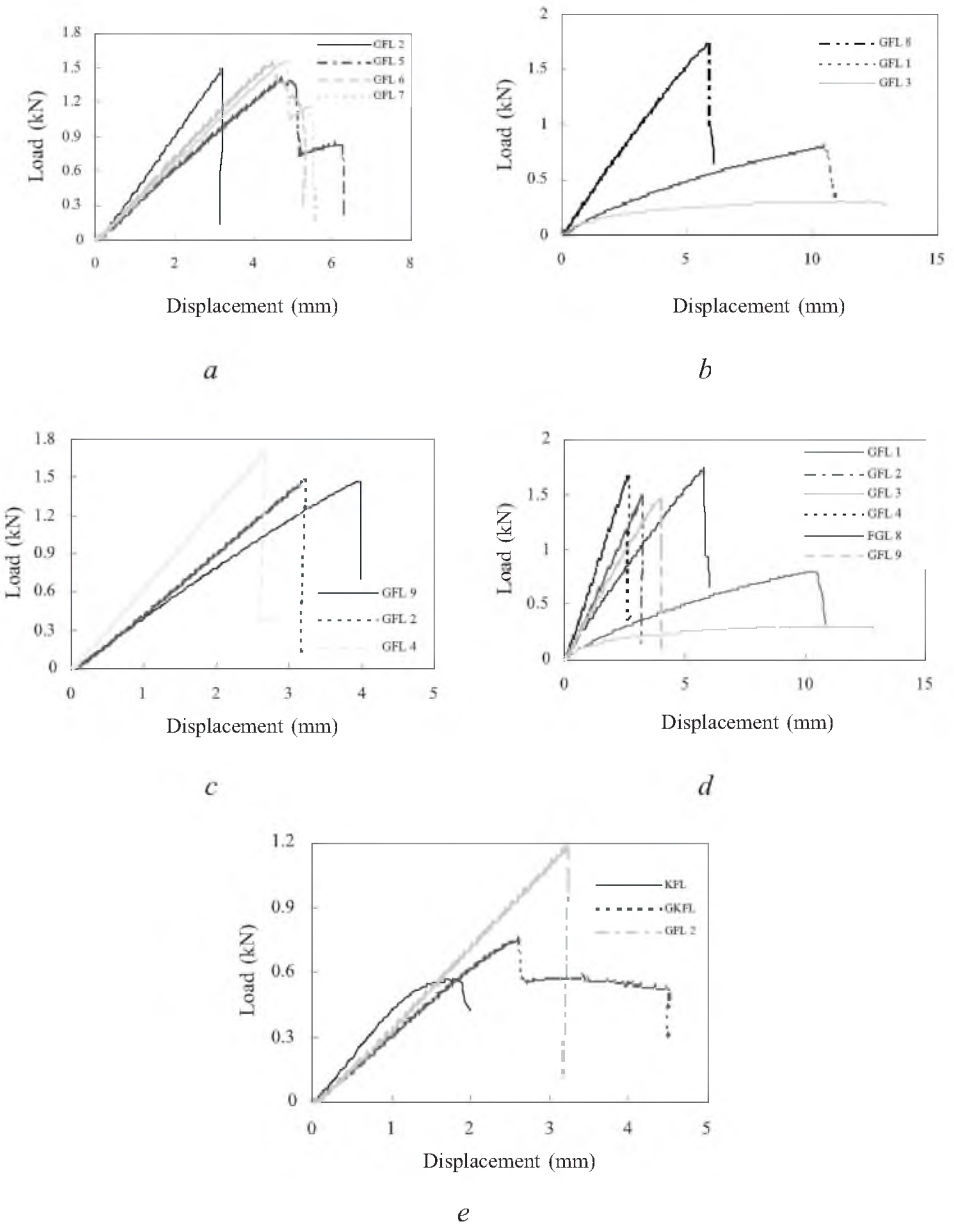

Fig. 2. Load evolution as a function of displacement in 3-point bending. The influence of stacking sequences (*a*), effects of thickness of 90°-oriented layers (*b*), effects of thickness of 0°-oriented layers (*c*), effects of disposition of 0°-oriented plies (*d*), and reinforcement type effects (*e*).

2.1.1. *Influence of Stacking Sequences*. The number of plies with the layers oriented at 0° and at 90° is the same (the ratio of the layer thickness equals to 1). The plies are piled up so that the thickness of the layers oriented at 90° is different between GFL 2 $(0_4/90_4)_s$, GFL 7 $[(0_2/90_2)_2]_s$, GFL 5 $[(0_2/90_2)_s]_s$ and GFL 6 $[(0/90)_4]_s$. It is clear from Fig. 2a that the GFL 2 laminate is more rigid than the three others, while its load and displacement at rupture are the lowest. This can be attributed to the cracks initiated on GFL 2, thus occupying a very large surface proportional to the thickness of the 90°-oriented layer (8 adjacent plies). Similar behavior was obtained for other materials GFL 5, GFL 6, and GFL 7.

2.1.2. *Effects of 90°-Oriented Layer Thickness*. To demonstrate the effect of the thickness of layers oriented at 90° and externally disposed in the laminate, we considered GFL 8 $(90_2/0_6)_s$, GFL 1 $(90_4/0_4)_s$, and GFL 3 $(90_6/0_2)_s$. Figure 2b shows that laminate GFL 8, with the smallest layer thickness oriented at 90° (2 plies), is the most rigid one, whose rupture load is the highest; followed by GFL 1 (4 plies) and then by GFL 3 (6 plies). In terms of displacement, the least rigid laminate GFL 3 has the largest displacement at rupture followed by GFL 1 and then GFL 8.

2.1.3. *Effects of 0°-Oriented Layer Thickness*. The laminates studied are GFL 9 $(0_2/90_6)_s$, GFL 2 $(0_4/90_4)_s$, and GFL 4 $(0_6/90_2)_s$. They all possess the same number of plies, with different thickness of layers oriented at 0° and externally disposed in the laminate. An increase in the thickness of 0°-oriented layers leads to an increase in both stiffness and load at rupture in bending and to a reduction in the displacement at rupture of the laminate as illustrated in Fig. 2c, which shows that the material of the largest 0°-oriented layer thickness (6 plies), GFL 4, is the most rigid with the weakest displacement at rupture, followed by GFL 2 (4 plies) and then GFL 9 (2 plies).

2.1.4. *Influence of the 0°-Oriented Layer Disposition*. The laminates are gathered by couples: GFL 9 $(0_2/90_6)_s$ and GFL 3 $(90_6/0_2)_s$, GFL 1 $(90_4/0_4)_s$ and GFL 2 $(0_4/90_4)_s$, and GFL 4 $(0_6/90_2)_s$ and GFL 8 $(90_2/0_6)_s$. Each couple has the same number of plies oriented at 0° and 90°, the difference lies in the layer disposition in the laminate (externally or internally oriented at 0°). Figure 2d shows that, for the above three couples, the laminates with the layers externally oriented at 0° are the most rigid but have the weakest displacements at rupture. As an example, we consider a couple of laminates GFL 9 and GFL 3, for which we note that (i) the laminate GFL 9 having the layers externally oriented at 0° is much more rigid than GFL 3, (ii) the load at rupture of the laminate GFL 9 is four times larger than that of GFL 3 while its displacement at rupture is three times less important.

2.1.5. *Influence of the Reinforcement Type*. In order to study the effect of the type of reinforcement on the stiffness and load and displacement at rupture, we considered the following laminates: (i) glass fiber GFL 2 $(0_{4G}/90_{4G})_s$; (ii) Kevlar fiber KFL $(0_{2K}/90_{2K})_s$, and (iii) hybrid glass and Kevlar fiber HGKFL $(0_{2G}/0_K/90_{2G}/90_K)_s$. The results obtained for these three laminates are shown in Fig. 2e. It is clear that the KFL laminate is the most rigid followed by GFL 2 and then HGKFL. It should also be noted that the presence of Kevlar fibers leads to a nonlinear behavior of the laminate, which is much more pronounced in the Kevlar laminate KFL.

2.2. **Observation of Rupture Topographies**. Optical and scanning electronic microscopes (SEM) have been used to observe the fracture topographies of the broken specimens after static tests; the obtained micrographs are illustrated in Fig. 3. This observation shows the presence of three types of damage, which lead to the total rupture of the laminate: (i) delamination between the layers oriented at 90° and those oriented at 0°, (ii) transverse cracking in the layers oriented at 90° and (iii) finally, rupture of fibers. Analysis of ruptures of various glass laminates, GFL 1 to GFL 9, in static tests allows us to classify them into two categories according to the disposition of the layers externally or internally oriented at 0° in the laminate:

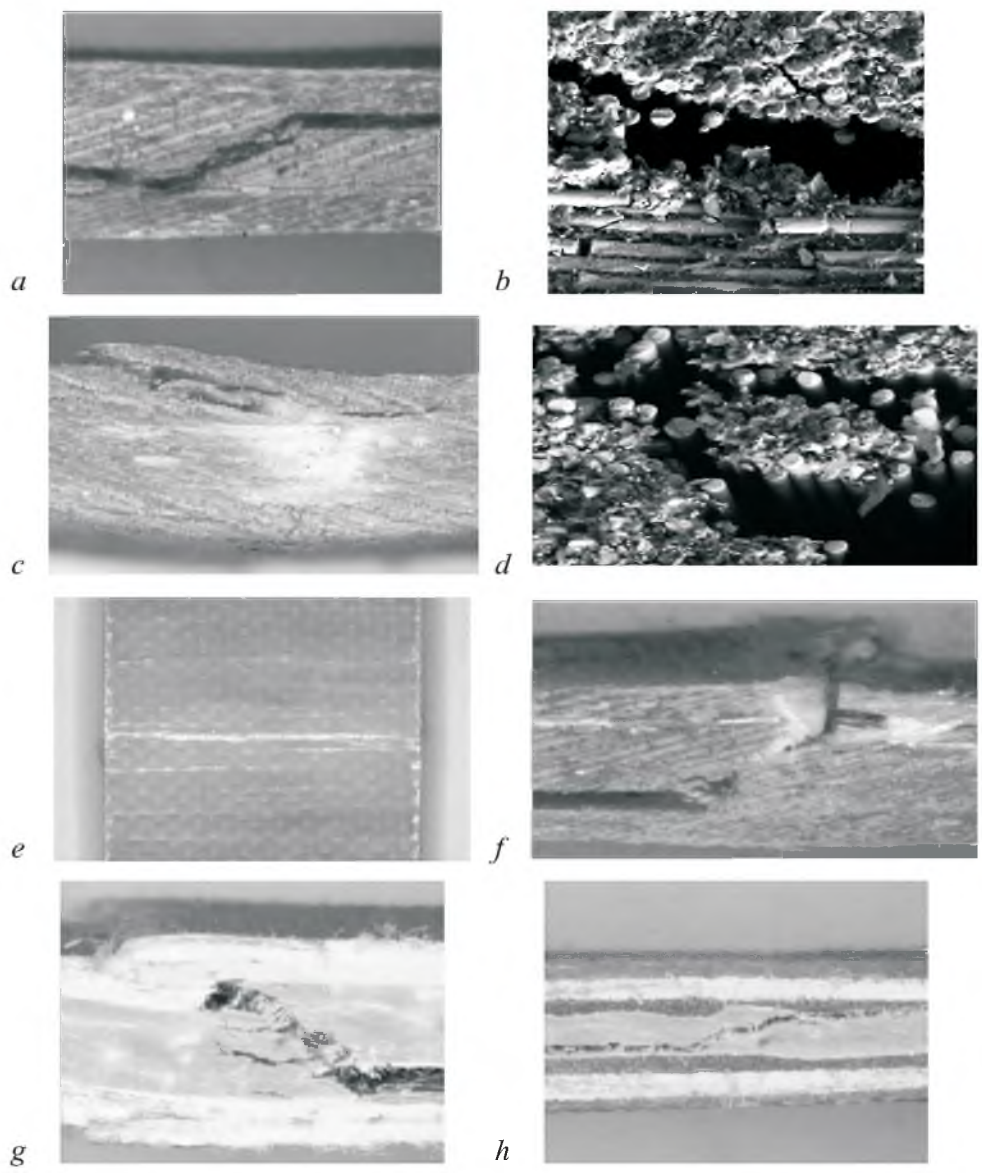

Fig. 3. Micrographs of different types of damage: optical (*a*, *c*, *e–h*) and SEM (*b*, *d*). (*a*, *b*) delamination and transverse crack; (*c*) delamination and rupture of compressed face; (*d*) transverse crack; (*e*) transverse crack in the tensile face; (*f*) delamination, transverse crack, and rupture of compressed face; (*g*) laminate KFL; (*h*) hybrid laminate HGKFL.

– *layers externally oriented at 0° in the laminate*: the specimens are little damaged by transverse cracking, whereas rupture is mainly due to delamination between the layers oriented at 0° and those at 90°. Beyond that, two cases of final rupture of the laminates are observed: (i) the externally oriented layers at 0° (Fig. 3a and 3b) remain without considerable damage in the laminates GFL 9 $(0_2/90_6)_s$, GFL 2 $(0_4/90_4)_s$, and GFL 4 $(0_6/90_2)_s$; these laminates of type $(0_n/90_m)_s$ consist of three layers, in which the one oriented at 90° has the largest thickness that favors delamination; and (ii) the externally oriented layers at 0° (Fig. 3f) of the compressed face break in the case of laminates GFL 5 $[(0_2/90_2)_s]_s$, GFL 6 $[(0/90)_4]_s$, and GFL 7 $[(0_2/90_2)_2]_s$. This can be explained by the fact that the thickness of the layers oriented at 90° is small since they are separated by layers oriented at 0°. In these two cases, brittle fracture of the laminates is observed as confirmed by the evolution of the load as a function of the displacement given in Fig. 2.

– *layers externally oriented at 90° in the laminate*: their damage (Fig. 3c and 3d) is mainly due to transverse cracking leading to rupture of fibers of the compressed face in the laminates GFL 8 $(90_2/0_6)_s$, GFL 1 $(90_4/0_4)_s$, and GFL 3 $(90_6/0_2)_s$. These laminates of type $(90_n/0_m)_s$ do not exhibit brittle fracture.

The presence of Kevlar fibers in the laminate changes the order of the occurrence of damage mechanisms as well as the rupture modes. For the Kevlar fiber laminate KFL $(0_{2K}/90_{2K})_s$ shown in Fig. 3g, one initially observes delamination between the lower layer (strained) oriented at 0° and the layer oriented at 90°, followed by transverse cracking that propagates in the layer oriented at 90° to reach the higher layer oriented at 0°. This crack leads to delamination of the above layer causing its rupture. For the hybrid glass-Kevlar fiber laminate HGKFL $(0_{2G}/0_K/90_{2G}/90_K)_s$ shown in Fig. 3h, brittle fracture was noted. This rupture is the result of delamination and transverse cracking in the Kevlar fiber layer oriented at 90°, while a glass fiber layer oriented at 90° seems not to be affected. This behavior can be explained by a poor Kevlar fiber-matrix epoxy adherence [27].

2.3. **Fatigue Tests**.

2.3.1. *Influence of Stacking Sequences on Fatigue Behavior*. During these tests, we recorded the evolution of the maximum load F as a function of the number of cycles N. The obtained results for various loading ratios R are shown in Figs. 4 and 5. The maximum load F is normalized by that obtained in the first cycle F_0. The description and analysis of such results (Fig. 4) show that the loss of load, F/F_0, extending until the rupture of the specimen, can be divided into three stages:

Stage I: corresponds to a sharp decrease, from the first cycles, in the ratio F/F_0 due to the cracking multiplication of the resin.

Stage II: shows a very slow decrease in the form of a shelf corresponding to almost the total fatigue life of the specimen due to a stable crack propagation.

Stage III: a very short stage wherein we observe again a sudden growth of damage until the total rupture of the specimen.

This behavior is in good agreement with the works of Talreja [11] and Muc [34] who distinguished three phases in the development of fatigue damage: in the first phase the matrix cracking, in the second the delamination or interfacial

debonding, and finally, the fiber breakage. It should be noted that the first stage is associated with less than 20% of the fatigue life but with about 80% of the damage ratio (F/F_0).

Figure 5 represents the development of the damage ratio F/F_0 as a function of the number of cycles for different stacking sequences of laminates GFL 5, GFL 6, GFL 7, and GFL 2 for various loading ratios R. Analysis of the results shows that under cyclic loading, the fatigue life depends on the loading ratio R and the stacking sequence.

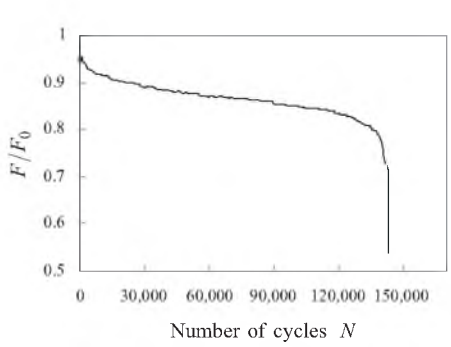

Fig. 4. A typical curve of rigidity evolution as a function of the number of cycles, N.

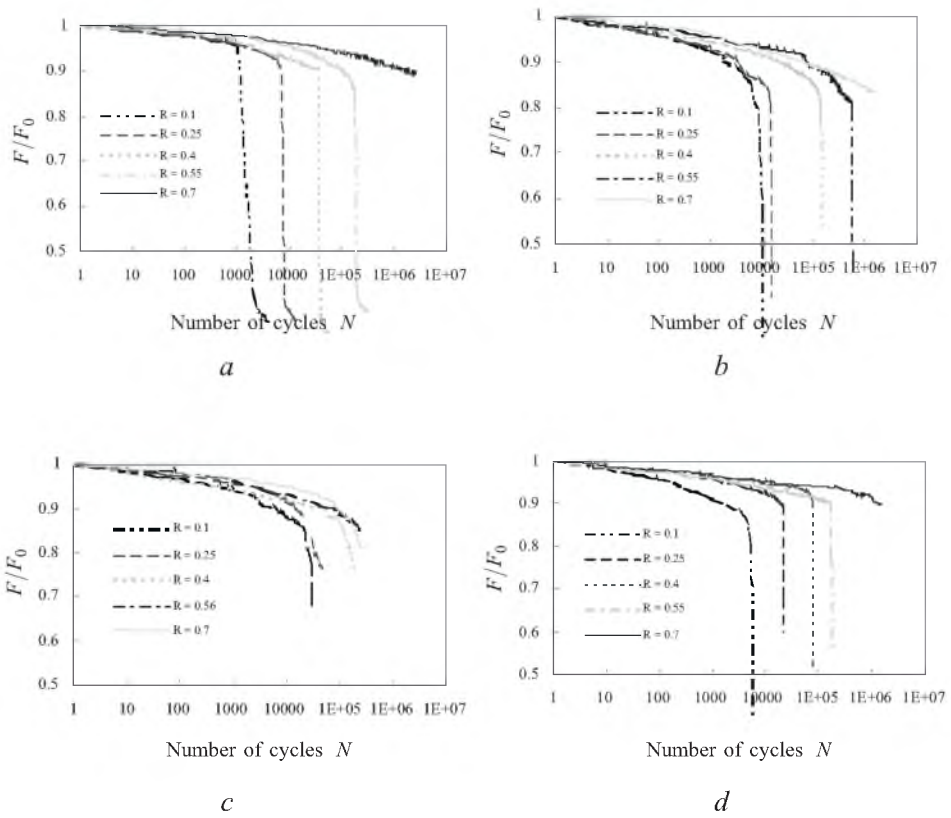

Fig. 5. Evolution of the rigidity loss, F/F_0, as a function of the number of cycles, N: (*a*) laminate GFL 2; (*b*) laminate GFL 5; (*c*) laminate GFL 6; (*d*) laminate GFL 7.

The average displacement determines the damage mechanisms activated at the beginning of cycling, while the amplitude determines the propagation velocity of the multiplication of these mechanisms. For the same maximum displacement, one notes for all laminates that: (i) for small R, corresponding to a large amplitude (weak average displacement), the initial damage is small with a considerably high growth rate leading to a very short fatigue life; the total rupture is quickly reached after only a few thousands of cycles; (ii) for large R, corresponding to a small amplitude (high average displacement), a lot of damage mechanisms are activated with a slow propagation, the fatigue life is very long and rupture is only partial even when the number of cycles is larger than 10^6.

To put into evidence the effects of stacking sequences on the fatigue resistance of the cross-ply laminates, we further compared (Fig. 6) the development of the load as a function of the number of cycles for three loading ratios ($R = 0.1$, 0.4, and 0.7). The results obtained show that the laminates having plies oriented at 90° bounded by those oriented at 0° have good resistance to fatigue in three-point bending.

In order to determine the performances of the materials in fatigue, various damage criteria (N_s, N_3, N_5, N_{10}, and N_R) are considered in the literature from the curves giving the evolution of the load as a function of the number of cycles. The most severe criterion is that characterizing the material by the value N_s, which corresponds to the number of cycles at the end of the linear domain. The criteria N_3, N_5, and N_{10} correspond to falls of 3%, 5%, and 10% of the load (or displacement) in relation to the initial load (or displacement), respectively. The criterion N_R corresponds to the number of cycles at the final rupture of the specimen. Finally, the performances in fatigue can be characterized by the number of cycles necessary to have rupture of the material when this number of cycles is reached. In our study, we have chosen the criterion N_{10}, which is the most frequently used one in the literature [7, 9, 15, 20]. Moreover, beyond 10%, a lot of mechanisms are involved and their description becomes more difficult, for example, for higher damage rates, the effect of local heating in the specimen cannot be neglected [9].

In Table 4, we summarize the obtained values of the fatigue life, using the criterion N_{10}, as functions of the ratio R for various laminates (GFL 5, GFL 6, GFL 7, and GFL 2) studied.

Table 4

Fatigue Life, N_{10}, as a Function of the Load Ratio, R, for Various Stacking Sequences

Laminates	Ratio R				
	0.1	0.25	0.4	0.55	0.7
GFL 2 $(0_4/90_4)_s$	$1.5 \cdot 10^3$	$0.65 \cdot 10^4$	$3.60 \cdot 10^4$	$1.02 \cdot 10^5$	$1.12 \cdot 10^6$
GFL 5 $[(0_2/90_2)_s]_s$	$2.5 \cdot 10^3$	$0.45 \cdot 10^4$	$2.15 \cdot 10^4$	$4.00 \cdot 10^5$	$1.40 \cdot 10^6$
GFL 7 $[(0_2/90_2)_2]_s$	$1.5 \cdot 10^3$	$1.80 \cdot 10^4$	$7.30 \cdot 10^4$	$1.67 \cdot 10^5$	$1.27 \cdot 10^6$
GFL 6 $[(0/90)_4]_s$	$5.0 \cdot 10^3$	$1.30 \cdot 10^4$	$4.80 \cdot 10^4$	$0.82 \cdot 10^5$	$0.95 \cdot 10^6$

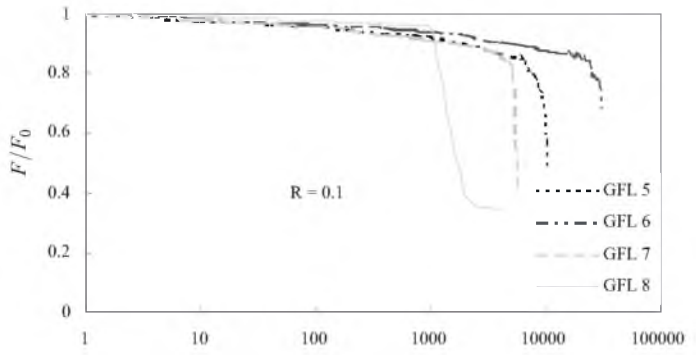

a

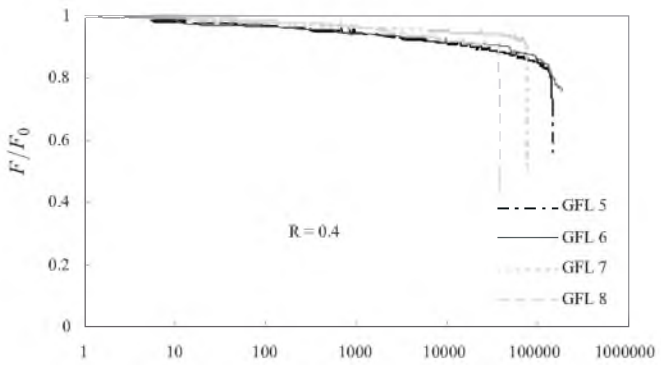

b

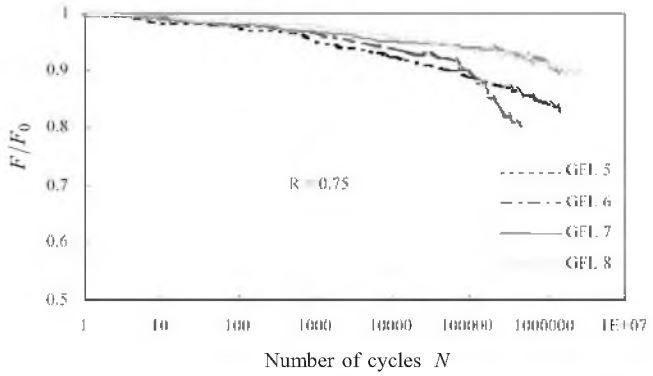

c

Fig. 6. Evolution of the rigidity loss, F/F_0, as a function of the number of cycles, N, at different loading ratios, R: (*a*) $R = 0.1$; (*b*) $R = 0.4$; (*c*) $R = 0.7$.

2.2.2. *Endurance Tests*. The evolution of stiffness is one of the most widely used methods to follow the development of damage by fatigue of composites. In the case of fatigue in bending with imposed displacement, a clear-cut rupture of a specimen is not generally observed. Therefore, the definition of the fatigue life rests on conventional criteria defined for a given rate of stiffness loss (N_{10} or

N_5). The fatigue life can be shown in a diagram of endurance giving the maximum level of the displacement or load as a function of the fatigue life (N_{10} or N_5).

In this part of our investigation, endurance tests are carried out in load control in the case of laminates GFL 2 $(0_4/90_4)_s$ and KFL $(0_{2K}/90_{2K})_s$ and in displacement control in the case of laminates GFL 2 and HGKFL $(0_{2G}/0_K/90_{2G}/90_K)_s$ with a 10 Hz frequency sinusoidal wave. The endurance curves are plotted for the load or displacement maximum as a function of the fatigue life N_{10} and N_5.

Figure 7 represents Wohler's curve for laminates GFL 2 and HGKFL. These results show the evolution of the maximum load normalized to the static rupture load as a function of the fatigue life N_{10}. In Fig. 8, we present Wцhler's curve for laminates GFL 2 and KFL, representing the evolution of the maximum displacement normalized to the static rupture displacement as a function of the fatigue life N_{10}.

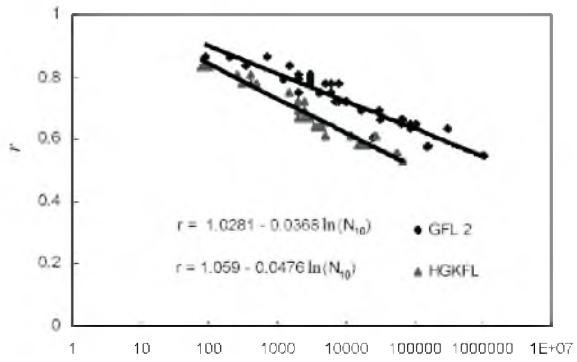

Fig. 7. $S-N$ curves for laminates GFL 2 and HGKFL in displacement control using N_{10} criterion.

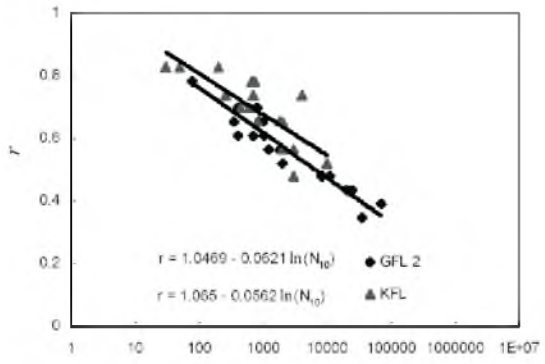

Fig. 8. $S-N$ curves of laminates GFL 2 and KFL in load control using N_{10} criterion.

Analysis of the obtained results shows the influence of reinforcement type on the fatigue life of laminates. Indeed, the Wohler curve of hybrid glass–Kevlar fiber (HGKFL) laminates lies below that of the glass-fiber laminate GFL 2 in displacement control (Fig. 7), whereas S–N curves for Kevlar-fiber laminates

(KFL) ones lie above those of the GFL 2 laminates (Fig. 8) in load control. The presence of Kevlar fibers in the laminate makes it more sensitive to fatigue in the case of 3-point bending and this can be explained by the poor fiber-matrix adherence [27].

Figure 9 represents endurance diagrams for the criteria of fatigue life N_{10} and N_5. The variation of the loading level r as a function of the number of cycles N can be described by a simple equation:

$$r = 1 - K \log N, \tag{1}$$

where K is the slope of the straight line of the fitted experimental data. This constant corresponds to the rate of decrease in the maximum load or the admissible maximum displacement expressed in % decrease per cycle. This form of representation allows us to show the influence of the reinforcement type and the criterion of fatigue life on the rate of independent deterioration of the control type. Indeed, the value of K is lower in the case of KFL and HGKFL laminates than that of GFL 2 laminate. The rate of deterioration increases with a decrease in the fatigue life criterion. We also notice that the evolution of the load or displacement loss with both methods of control and in both cases of fatigue life crosses the axis at about $r = 1$ that corresponds to the loading level equal to that of the static rupture.

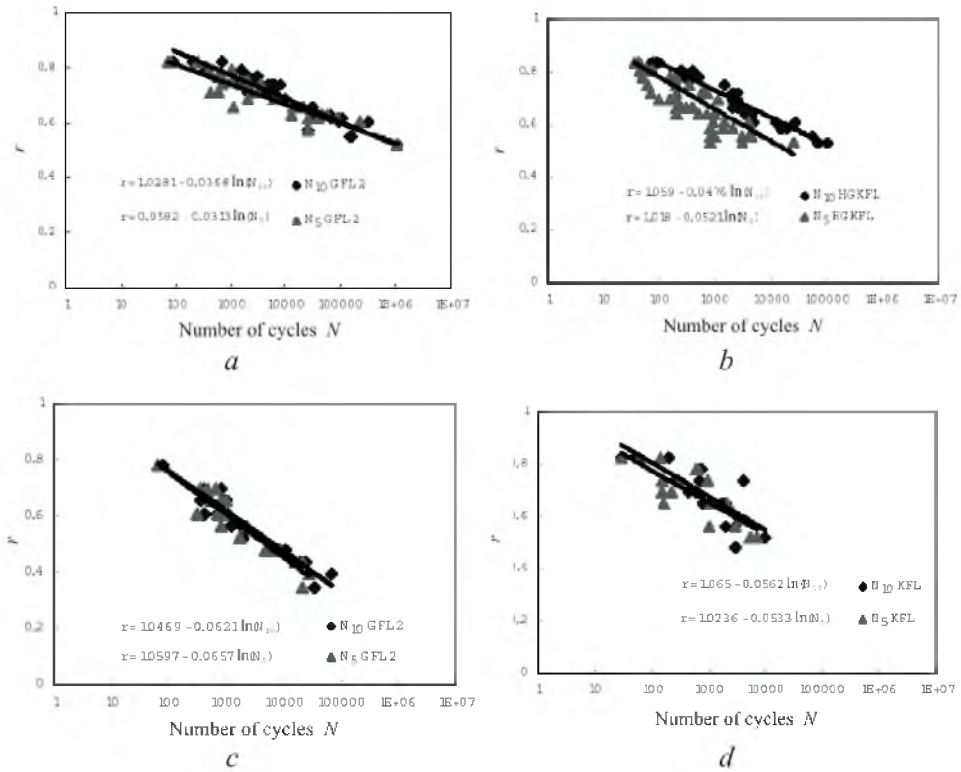

Fig. 9. $S-N$ curves for both modes of control using N_5 and N_{10} criteria: (*a*) displacement control for GFL 2 laminate; (*b*) displacement control for hybrid HGKFL laminate; (*c*) load control for GFL 2 laminate; (*d*) load control for hybrid HGKFL laminate.

It should be noted that endurance tests are characterized by dispersion of fatigue life values depending on the reinforcement type in the laminate. Indeed, the tests on the Kevlar fiber laminate are characterized by an appreciable dispersion of fatigue life values as compared to other laminates. Generally, this dispersion may be attributed to the heterogeneous nature of the laminates. Moreover, specimens do not always have the same characteristics: volume fraction, defect distribution, strength at static rupture, etc. Fatigue rupture depends on random processes whose combination results in dispersion of the fatigue life values between the specimens subjected to the same loading level r. Furthermore, it is worth noting that both dispersion and rupture criteria have the same trend.

Conclusions. This investigation deals with an experimental approach involving the mechanical behavior of different Kevlar- and glass-fiber cross-ply laminates with epoxy resin in three-point bending under static and fatigue loading. Static study showed the influence of the stacking sequence, the thickness effect of the layers oriented at 0° and 90°, their internal or external disposition in the laminate, and the reinforcement type on the values of the load and displacement at rupture of the laminates.

Analysis of the observed fracture topographies of specimens broken in static investigations via optical and SEM techniques made it possible to classify rupture as a function of the internal or external disposition of the layers oriented at 0° in the laminate:

For glass-fiber laminates of type $(0_n/90_m)_s$, brittle fracture has been observed. The specimens are little damaged by transverse cracking with the rupture of the laminate caused by delamination with and without rupture of the compressed face. However, for KFL and HKGFL, non-brittle rupture was obtained mainly because of the presence of Kevlar fibers.

For the laminates of type $(90_n/0_m)$, damage is mainly due to transverse cracking in the 90° externally oriented layers leading to rupture of the fibers of the compressed face. This type of damage, inducing non-brittle rupture, is observed in the laminates.

The influence of the stacking sequence on the fatigue behavior has been studied by considering four types of laminates for several loading ratios R in displacement control. The loading level r has been considered constant and equal to 60% of the displacement at rupture. Analysis of these results shows that (i) the behavior and the fatigue life depends on the ratio R and (ii) the laminates whose plies are oriented at 90° and separated by those at 0° resist better to fatigue. Indeed, the fatigue life N increases with R.

Wцhler's curves are obtained by using the fatigue life criteria N_5 and N_{10} in load control for laminates GFL 2 and KFL, and in displacement control for laminates GFL 2 and HKGFL. It is noticed that in the case of load control, damage of the laminates is more pronounced than that in displacement control. Glass fiber laminates GFL 2 resist better to fatigue than HKGFL laminates in displacement control, whereas they seem to be less resistant to fatigue than the KFL laminates in load control. The presence of the Kevlar fiber in the laminate makes it more sensitive to fatigue in three-point bending that can be attributed to the poor fiber–matrix adherence [27].

Rupture in fatigue depends on a series of random processes leading to dispersed results due to the heterogeneous nature of the laminates and manufacturing. Despite dispersions, which is more pronounced in load control, particularly for the Kevlar fiber laminate KFL, the analysis of these results shows clearly the influence of the reinforcement type on the fatigue life of the laminates studied.

The evolution of the loading level r as a function of the logarithm of the fatigue life N is described by the same relationship $r = 1 - K \log N$, thus showing the influence of the reinforcement type and the fatigue life criterion on the rate of degradation.

Acknowledgements. I would like to thank Professors A. Dogmane, B. Bencer, and A. Haddad.

Резюме

У рамках експериментального підходу описано механічну поведінку різних ламінатів із матрицею з епоксидної смоли, що перехресноармовані кевларовими волокнами і скловолокнами, в умовах статичного і циклічного триточкового згину. При статичних випробуваннях розглядаються послідовність укладення шарів і волокон, товщини орієнтованих під кутом 90° шарів і вплив типу армування на механічну поведінку ламінатів у процесі навантаження, а також на реалізацію різних режимів пошкодження, що призводить до руйнування. Дослідження при циклічному навантаженні складається з двох етапів. На першому етапі розглядається вплив послідовності укладення шарів і волокон на поведінку і довговічність чотирьох типів армованих скловолокнами ламінатів, на другому етапі – вплив типу армування на циклічну міцність і опір ламінатів при циклічному навантаженні. Випробування на втому виконано у м'якому режимі навантаження для армованих скловолокнами і гібридними волокнами (кевлар + скло) ламінатів. На основі критеріїв зниження жорсткості на 5 і 10% в координатах напруження – число циклів до руйнування побудовано криві утоми. Аналіз отриманих результатів дозволяє оцінити вплив послідовності укладення шарів і типу армування на поведінку перехресноармованих ламінатів при циклічному навантаженні. Наявність кевларових волокон у ламінатах запезчує їх нелінійну поведінку при статичних випробуваннях і низьку циклічну міцність при випробуваннях на втому в умовах триточкового згину.

1. C. K. H. Dharan, "Fatigue failure in graphite fibers and glass fibers-polymer composites," *J. Mater. Sci.*, **10**, 1665–1670 (1975).
2. J. Awerbuch and H. T. Hahn, "Fatigue of filamentary composite materials," in: *ASTM STP 636* (1977), pp. 248–266.
3. H. T. Hahn and L. Lorenzo, "Fatigue failure mechanisms in composite laminates. Advances in fracture research," in: Proc. 6th Inter. Conf. on Fracture (New Delhi, India, 4–10 Dec.) (1984), pp. 549–568.
4. J. F. Mandell, "Fatigue behavior of fiber resin composites, developments in reinforced plastics," in: G. Pritchard (Ed.), Applied Science Publishers, London, New York (1982), pp. 67–107.

5. R. Talreja, "Fatigue of composite materials: damage mechanisms and fatigue-life diagrams," *Proc. Roy. Soc. London*, **A(378)**, 461–475 (1981).
6. H. C. Kim and L. J. Ebert, "Fatigue life limiting parameters in fiber glass composites," *J. Mater. Sci.*, **14**, 2616–2624 (1979).
7. A. Djebbar, F. Sidoroff, et L. Vincent, "Etude du couplage traction-cisaillement dans le cas de sollicitations en flexion de matériaux composites verre/époxyde," *Journée Nationale des Composites (JNC)*, 7 Nov., 81–90 (1990).
8. M. Dody, *Modélisation des Caractéristiques Mécaniques et Études Expérimentales de l'Endommagement d'un Composite*, Ph. D. Thesis, Université de Franche-Comté, Besançon, France (1985).
9. L. Fiore, *Contribution à l'Étude du Comportement en Fatigue de Matériaux Composites à Renfort Verre Unidirectionnel*, Ph. D. Thesis, Ecole Centrale de Lyon, France (1988).
10. J.-M. Berthelot, P. Leblond, A. El Mahi, and J.-F. Le Corre, "Transverse cracking of cross-ply laminates. Part 1. Analysis," *J. Compos.*, **27A**, 989–1001 (1996).
11. R. Talreja, *Fatigue of Composite Materials*, Lancaster Technol. Publishing, (1990).
12. J.-M. Berthelot, "Analysis of the transverse cracking of cross-ply laminates: a generalized approach," *J. Compos. Mater.*, **31**, 1780–1805 (1997).
13. A. D'amore, G. Caprino, R. Stupak, J. Zhou, and L. Nicolais, "Effect of stress ratio on the flexural fatigue behavior of continuous stand mat reinforced plastics," *J. Sci. Eng. Compos. Mater.*, **5** (1), 1–8 (1996).
14. J. Li, B. Zhou, and T. He, "Residual properties of an infection-molded poly (phenylene enther ketone)/carbon composite during flexural fatigue," *J. Compos. Sci. Technol.*, **57**, 669–676 (1997).
15. M. Salvia, L. Fiore, P. Fournier, and L. Vincent, "Flexural fatigue behavior of UDGFRP – experimental approach," *Int. J. Fatigue*, **19** (3), 253–262 (1997).
16. A. Salaün, *Etude de l'Endommagement en Flexion 3 Points et en Flambage de Composites Carbone/Époxy 1D et 2D à Plis Croisés*, Ph. D. Thesis, Université de Caen, France (1998).
17. A. Salaün and M. Gomia, "Static fatigue and cyclic behavior of unidirectional carbon/epoxy," *J. Compos. Ann. Chim. Sci. Mater.*, **23**, 19–22 (1998).
18. G. Caprino and G. Giorleo, "Fatigue lifetime of glass fiber/epoxy composites," *J. Compos.*, **30A**, 299–304 (1999).
19. L. V. Griffin, J. C. Gibeling, R. B. Martin, V. A. Gibson, and S. M. Stover, "The effects of testing methods on the flexural fatigue life of human cortical bone," *J. Biomech.*, **30**, 105–109 (1999).
20. S. Tamboura, H. Sidhom, et H. P. Lieurade, "Matériau composite à fibers de carbone et matrice époxyde: étude du mécanisme d'endommagement," *Matériau et Techniques*, Nos. 3–4, 15–20 (1996).

21. M. G. Stout, D. A. Koss, C. Liu, and J. Idasetima, "Damage development in carbon/epoxy laminates under quasi-static and dynamic loading," *Compos. Sci. Technol.*, **59**, 2339–2350 (1999).
22. N. J. Lee, K. E. Fu, and J. N. Yang, "Prediction of fatigue damage and life for composite laminates under service loading spectra," *Compos. Sci. Technol.*, **56**, 635–648 (1996).
23. J. A. M. Ferreira, J. D. M. Costa, P. N. B. Reis, and M. O. W. Richardson, "Analysis of fatigue and damage in glass-fiber reinforced polypropylene composite materials," *Compos. Sci. Technol.*, **59**, 1461–1467 (1999).
24. A. El Mahi, A. R. Bezazi, and J.-M. Berthelot, "The fatigue behavior and damage development in cross-ply laminates in flexural tests," in: Proc. Tenth European Conf. on *Composite Materials* (ECCM-10), Bruge, Belgium (3–5 June, 2002).
25. A. R. Bezazi, A. El Mahi, J. -M. Berthelot, and B. Bezzazi, "Influence of reinforcement in cross-ply laminates in flexural testing," in: Proc. Conf. *New Trends in Fatigue and Fracture*, Metz, France (8–9 April, 2002).
26. A. R. Bezazi, A. El Mahi, J.-M. Berthelot, et B. Bezzazi, "Analyse de l'endommagement des stratifiés en flexion 3-points. Influence de la séquence d'empilement," in: Proc. XVème Congrès Francais de Mécanique, Nancy, France (3–7 Septembre, 2001).
27. J.-M. Berthelot, *Composite Materials. Mechanical Behavior and Structural Analysis*, Springer, New York (1999).
28. R. H. Ericksen, "Room temperature creep of Kevlar 49/epoxy composites," *Compos.*, **6** (1976).
29. M. R. Piggott and B. Harris, "Compression strength of carbon, glass, and Kevlar 49 fiber reinforced polyester resins," *J. Mater. Sci.*, **15**, 2523–2538 (1980).
30. B. Harris, J. Adam, et H. Reiter, "Composites hybrides carbone–Kevlar et carbone-verre, comportement en fatigue," *Journée Nationale des Composites* (JNC), *6*, 649–660 (1988).
31. S. M. Bleay and L. Humbertone, "Mechanical and electrical assessment of hybrid composites containing hollow glass reinforcement," *Compos. Sci. Technol.*, **59**, 1321–1329 (1999).
32. A.-K. Akbar, L. Glyn, Y. Lin, and M. Yiu-Wing, "On the fracture mechanical behavior of fiber reinforced metal laminates (FRMLs)," in: *Comp. Meth. Appl. Mech. Eng.*, **185**, 173–190 (2000).
33. Y. Shan and K. Liao, "Environmental fatigue of unidirectional glass-carbon fiber reinforced hybrid composite," *Compos.*, Part B, **32**, 355–363 (2001).
34. A. Muc, "Design of composite structures under cyclic loads," *Comp. Struct.*, **76**, 211–218 (2000).
35. A. Laksimi, A. Benyahia, M. L. Benzeggagh, and X. L. Gong, "Initiation and bifurcation mechanisms of cracks in multi-directional laminates," *Compos. Sci. Technol.*, **60**, 597–604 (2000).

36. R. Olsson, J. C. Thesken, F. Brandt, N. Jönsson, and S. Nilsson, "Investigations of delamination criticality and the transferability of growth criteria," *Compos. Struct.*, **36**, 221–247 (1996).
37. K.-L. Choy, P. S. Rogers, D. Churchman, and M. T. Pirzada, "The mechanical behavior of glass-ceramic matrix composites," *Mater. Sci. Eng.*, **A278**, 187–194 (2000).
38. H. Plumtree and G. X. Cheng, "Fatigue parameter for off-axis unidirectional fiber reinforced composites," *Int. J. Fatigue*, **21**, 844–856 (1999).
39. L. Andre, L. Kenneth, et al. "Prediction of stress-rupture life of glass/epoxy laminates," *Int. J. Fatigue*, **22**, 467–480 (2000).
40. J.-M. Berthelot, and J.-F. Le Corre, "Modeling the transverse cracking in cross-ply laminates: application to fatigue," *J. Compos.*, **30B**, 569–577 (1999).
41. J.-M. Berthelot and J.-F. Le Corre, "Statistical analysis of the progression of transverse cracking and delamination in cross-ply laminates," *Compos. Sci. Technol.*, **60**, 2659–2669 (2000).
42. J.-M. Berthelot and J.-F. Le Corre, "A model for transverse cracking and delamination in cross-ply laminates," *Compos. Sci. Technol.*, **60**, 1055–1066 (2000).
43. J.-M. Berthelot, A. El Mahi, and J. F. Le Corre, "Development of transverse cracking in cross-ply laminates during fatigue tests," *Compos. Sci. Technol.* (2001), *to appear*.

Received 21. 10. 2002